

Electronic Structure of the  $\alpha$  and  $\beta$  Isomers Of  $[\text{Mo}_8\text{O}_{26}]^{4-}$ Adam J. Bridgeman\*<sup>†</sup> and Germán Cavigliasso<sup>†,‡</sup>*Department of Chemistry, University of Hull, Kingston upon Hull HU6 7RX, U.K., and  
Department of Chemistry, University of Cambridge, Lensfield Road, Cambridge CB2 1EW, U.K.*

Received February 20, 2002

The structure and bonding in  $\alpha$  and  $\beta$  octamolybdate anions have been investigated using density functional methods. In general, good computational–experimental agreement for the geometrical parameters has been obtained. The electronic structure of the anions has been probed with molecular orbital and Mulliken–Mayer methods. All Mo–O interactions have been found to be predominantly d(Mo)–p(O) in character. Several multicentered molecular orbitals can be described as  $\sigma$  or  $\pi$  closed-loop structures, but the proposed connection with the stability of the polyanions is not completely supported by the calculations. Mayer indexes correspond to fractional multiple character for terminal bonds and approximately single or low-order character for bridging bonds, in accordance with structural and bond valence results. The valency analysis has yielded similar overall bonding capacity for the various oxygen atoms. A distribution of the negative charge over all types of oxygen sites and metal charges considerably smaller than the formal oxidation states have been obtained from the Mulliken analysis.

## Introduction

The structures of polyoxometalates can be characterized as an assemblage of  $\text{MO}_n$  coordination polyhedra, linked through the sharing of corners, edges, and rather infrequently faces, in which the metal atoms are displaced toward the vertices that lie at the surface of the clusters.<sup>1,2</sup> In the most typical isopoly and heteropoly species, distorted  $\text{MO}_6$  octahedra are the primary constituent units.

An interesting structural feature of polyoxoanions is the occurrence of interpenetrating closed loops, formed by the metal centers and the bridging oxygen atoms linking the octahedral units, that have been regarded as a type of macrocyclic bonding system constructed via multicentered  $\sigma$  and  $\pi$  interactions.<sup>3–8</sup> Nomiya and Miwa<sup>3</sup> have proposed a connection between the structural stability of polyoxometalates and the number of closed loops per  $\text{MO}_6$  octahedron in the form of an index ( $\eta$ ) defined as

$$\eta = \frac{\sum BC}{A} \quad (1)$$

where  $A$  is the number of octahedra constituting the polyanion cage,  $B$  is the number of  $\text{MO}_6$  units constituting the closed loop, and  $C$  is the number of closed loops. It should be noted that the polyanion cage is not necessarily identical with the whole structure, although it does comprise most of it.<sup>3</sup>

Nomiya and Miwa have considered that structures with a higher  $\eta$  value should be more stable, but they have sometimes needed to invoke additional factors in cases where this idea does not seem to work.<sup>3–7</sup> For both the  $\alpha$  and  $\beta$  forms of the octamolybdate anion, a value of 1 has been proposed for the respective indexes suggesting that, in principle, these isomers may exhibit comparable stability.

In this article, we report the results of density functional calculations on  $\alpha$  and  $\beta$   $[\text{Mo}_8\text{O}_{26}]^{4-}$  isopolyanions. The molecular structures of both isomers have been fully optimized, and the electronic structures have been analyzed by a combination of molecular orbital, population, and bonding energy methods. The orbital properties of the metal–oxygen closed loops and the connection to the stability of the clusters are also explored and described.

## Computational Approach

All density functional calculations reported in this work were performed with the ADF<sup>9,10</sup> or GAMESS-UK<sup>11</sup> programs. Func-

\* Corresponding author. E-mail: A.J.Bridgeman@hull.ac.uk. Phone: +44 1482 466549. Fax: +44 1482 466410.

<sup>†</sup> University of Hull.

<sup>‡</sup> University of Cambridge.

- (1) Pope, M. T. *Heteropoly and Isopoly Oxometalates*; Springer-Verlag: Heidelberg, Germany, 1983.
- (2) Pope, M. T.; Müller, A. *Angew. Chem., Int. Ed. Eng.* **1991**, *30*, 34.
- (3) Nomiya, K.; Miwa, M. *Polyhedron* **1984**, *3*, 341.
- (4) Nomiya, K.; Miwa, M. *Polyhedron* **1985**, *4*, 89.
- (5) Nomiya, K.; Miwa, M. *Polyhedron* **1985**, *4*, 675.
- (6) Nomiya, K.; Miwa, M. *Polyhedron* **1985**, *4*, 1407.
- (7) Nomiya, K. *Polyhedron* **1987**, *6*, 309.
- (8) King, R. B. *Inorg. Chem.* **1991**, *30*, 4437.

tionals based on the Vosko–Wilk–Nusair (VWN)<sup>12</sup> form of the local density approximation (LDA),<sup>13</sup> and on a combination (labeled BP86) of Becke's 1988 exchange<sup>14</sup> and Perdew's 1986 correlation<sup>15</sup> corrections to the LDA, and Slater-type-orbital (STO) basis sets of triple- $\zeta$  quality incorporating frozen cores and the ZORA relativistic approach (ADF O.1s and Mo.3d type IV)<sup>9,10</sup> were utilized in ADF calculations. The B3LYP<sup>16</sup> functional and Gaussian-type-orbital (GTO) basis sets of double- $\zeta$  quality and of the effective-core-potential type<sup>17–19</sup> were employed in GAMESS-UK calculations.

The functional and basis set choices were based on the results of tests performed on several  $[\text{MO}_4]$  and  $[\text{M}_2\text{O}_7]$  species.<sup>20,21</sup> Geometry optimizations were carried out using LDA methods, and data on thermochemistry and energetics were extracted from single-point BP86 or B3LYP calculations. Bond and valency indexes were obtained according to the definitions proposed by Mayer<sup>22,23</sup> and by Evarestov and Veryazov,<sup>24</sup> with a program<sup>25</sup> designed for their calculation from the ADF output file. Graphics of molecular orbitals were generated with the MOLEKEL<sup>26</sup> program.

## Results and Discussion

**Molecular Structures.** Structural and atom-labeling schemes for the  $\alpha$  and  $\beta$  isomers are presented in Figure 1a,b, respectively. The optimized molecular geometries are given in Table 1, which also includes experimental data taken from the compilations of Tytko and co-workers.<sup>27</sup> These results correspond to  $D_{3d}$  ( $\alpha$ ) or  $C_{2h}$  ( $\beta$ ) averages of bond parameters in crystal structures.

The  $\alpha$  form consists of a "ring" of six (distorted)  $[\text{MoO}_6]$  octahedra bicapped by (distorted)  $[\text{MoO}_4]$  tetrahedra. The six-coordinate Mo ( $\text{Mo}_{6c}$ , M6) atoms are bonded to two unshared oxygen (O6) atoms, whereas the four-coordinate Mo ( $\text{Mo}_{4c}$ , M4) centers are involved in one terminal (M4–O4) bond. The bridging sites are represented by two-

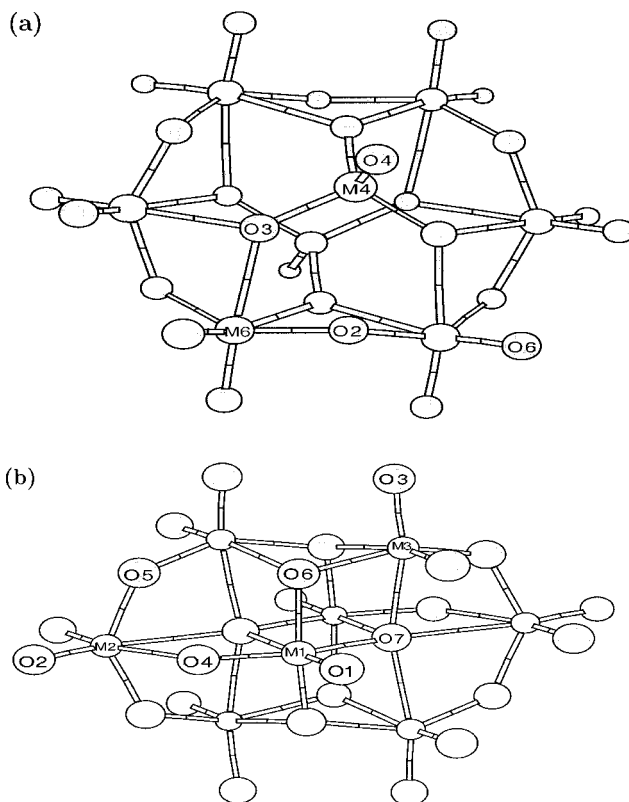


**Figure 1.** Structural and atom-labeling schemes for (a)  $\alpha$  and (b)  $\beta$   $[\text{Mo}_8\text{O}_{26}]^{4-}$  anions.

**Table 1.** Optimized Mo–O Bond Distances for the  $\alpha$  and  $\beta$  Isomers of  $[\text{Mo}_8\text{O}_{26}]^{4-}$

isomer	parameter	calcd	expt	
$\alpha$	$\text{Mo}_{4c}\text{--O}_t$	M4–O4	174	171
	$\text{Mo}_{6c}\text{--O}_t$	M6–O6	172	169
	$\text{Mo}_{6c}\text{--O}_{2c}$	M6–O2	192	191
	$\text{Mo}_{4c}\text{--O}_{3c}$	M4–O3	180	178
	$\text{Mo}_{6c}\text{--O}_{3c}$	M6–O3	240	244
$\beta$	$\text{Mo--O}_t$	M1–O1	172	170
		M2–O2	174	170
		M3–O3	173	170
	$\text{Mo--O}_{2c}$	M1–O4	178	175
		M2–O4	220	229
		M2–O5	192	193
		M3–O5	191	189
	$\text{Mo--O}_{3c}$	M1–O6	196	195
		M3–O6	198	200
		M3–O6	235	235
	$\text{Mo--O}_{5c}$	M1–O7	208	215
		M1–O7	238	238
		M2–O7	256	245
	M3–O7	235	232	

coordinate oxygen ( $\text{O}_{2c}$ , O2) atoms that form an  $[\text{Mo}_6\text{O}_6]$  closed loop, or by three-coordinate oxygen ( $\text{O}_{3c}$ , O3) atoms that provide both  $\text{Mo}_{6c}\text{--O--Mo}_{4c}$  and  $\text{Mo}_{6c}\text{--O--Mo}_{6c}$  connections.

In the  $\beta$  form, all Mo atoms are six-coordinate but are not equivalent. Three distinct metal centers are found and have been labeled M1, M2, and M3. The oxygen sites fall broadly into four categories, terminal ( $\text{O}_t$ : O1, O2, O3), two-coordinate ( $\text{O}_{2c}$ : O4, O5), three-coordinate ( $\text{O}_{3c}$ : O6), and five-coordinate ( $\text{O}_{5c}$ : O7) atoms, but as the labels suggest, there are also individual differences in the  $\text{O}_t$  and  $\text{O}_{2c}$  groups. The O4 atoms constitute a special case. Although these are

- (9) ADF2000.02: Baerends, E. J.; Ellis, D. E.; Ros, P. *Chem. Phys.* **1973**, 2, 41. Versluis, L.; Ziegler, T. *J. Chem. Phys.* **1988**, 322, 88. te Velde, G.; Baerends, E. J. *J. Comput. Phys.* **1992**, 99, 84. Fonseca Guerra, G.; Snijders, J. G.; te Velde, G.; Baerends, E. J. *Theor. Chem. Acc.* **1998**, 99, 391.
- (10) te Velde, G.; Bickelhaupt, F. M.; Baerends, E. J.; FonsecaGuerra, C.; van Gisbergen, S. J. A.; Snijders, J. G.; Ziegler, T. *J. Comput. Chem.* **2001**, 22, 931.
- (11) Guest, M. F.; van Lenthe, J. H.; Kendrick, J.; Schöffel, K.; Sherwood, P.; Amos, R. D.; Buenker, R. J.; Dupuis, M.; Handy, N. C.; Hillier, I. C.; Knowles, P. J.; Bonacic-Koutecky, V.; von Niessen, W.; Harrison, R. J.; Rendell, A. P.; Saunders, V. R.; Stone, A. J. *GAMESS-UK*, version 6; Daresbury Laboratory: Warrington, England.
- (12) Vosko, S. H.; Wilk, L.; Nusair, M. *Can. J. Phys.* **1980**, 58, 1200.
- (13) Kohn, W.; Sham, L. J. *Phys. Rev.* **1965**, 140, A1133.
- (14) Becke, A. D. *Phys. Rev. A* **1988**, 38, 3098.
- (15) Perdew, J. P. *Phys. Rev. B* **1986**, 33, 8822.
- (16) Stephens, P. J.; Devlin, F. J.; Chabalowski, C. F.; Frisch, M. J. *J. Phys. Chem.* **1994**, 98, 11623.
- (17) Stevens, W. J.; Basch, H.; Krauss, M. *J. Chem. Phys.* **1984**, 81, 6026.
- (18) Stevens, W. J.; Jasien, P. G.; Krauss, M.; Basch, H. *Can. J. Chem.* **1992**, 70, 612.
- (19) Cundari, T. R.; Stevens, W. J. *J. Chem. Phys.* **1993**, 98, 5555.
- (20) Bridgeman, A. J.; Cavigliasso, G. *Polyhedron* **2001**, 20, 2269.
- (21) Bridgeman, A. J.; Cavigliasso, G. *J. Phys. Chem. A* **2001**, 105, 7111.
- (22) Mayer, I. *Chem. Phys. Letters* **1983**, 97, 270.
- (23) Mayer, I. *Int. J. Quantum Chem.* **1984**, 26, 151.
- (24) Evarestov, R. A.; Veryazov, V. A. *Theor. Chim. Acta* **1991**, 81, 95.
- (25) Bridgeman, A. J. *MAYER*; a program to calculate Mayer bond-order indexes from the output of the electronic structure packages GAMESS–UK, GAUSSIAN, and ADF; University of Hull: Hull, U.K., 2001. Available from the author on request.
- (26) *MOLEKEL: An Interactive Molecular Graphics Tool*; Portmann S.; Lüthi, H. P. *Chimia* **2000**, 54, 766.
- (27) Tytko, K. H.; Mehmke, J.; Fischer, S. *Struct. Bonding (Berlin)* **1999**, 93, 129.

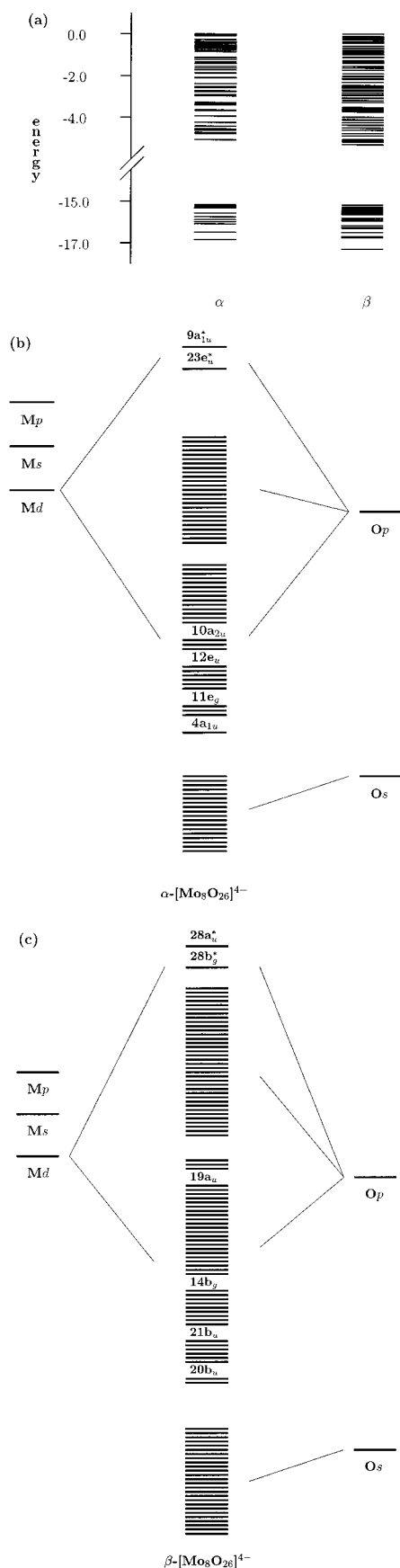


**Figure 2.** Electronic structure of  $\alpha$  and  $\beta$  isomers: (a) eigenvalue (eV) diagram for the occupied valence levels (highest-occupied level is used as reference), (b) and (c) qualitative molecular orbital diagram showing predominant metal and oxygen contributions to the occupied and lowest virtual valence levels.

formally two-coordinate sites, the M1–O4 and M2–O4 distances (Table 1) are more typical of bonds to terminal and high-coordinate O atoms, respectively, than they are of a “normal” Mo–O<sub>2c</sub> bond. Therefore, the O4 sites in the  $\beta$  isomer have sometimes been considered in a separate category and have been classified as pseudoterminal (O<sub>pt</sub>) oxygen atoms.<sup>27</sup>

The computational–experimental agreement is, in general, reasonably good for both isomers. The present calculations correspond to isolated gas-phase molecules and are thus not directly comparable to solid-state data. Nevertheless, experimental data for all types of Mo–O bonds are well reproduced by the calculations for the  $\alpha$  form. This observation also applies to the  $\beta$  form, with the exception of three parameters (M2–O4, M1–O7, M2–O7 distances) for which the deviations are rather noticeable. These three cases fall into the group of longest and (presumably) weakest Mo–O bonds.

**Electronic Structures. Molecular Orbital Diagrams.** Eigenvalue diagrams for the occupied valence levels of the  $\alpha$  and  $\beta$  isomers and qualitative molecular orbital schemes showing predominant metal and oxygen contributions are given in Figure 2. It should be noted that the latter are entirely qualitative, and no accurate quantitative correlation exists among the positions of the atomic and molecular energy levels. These schemes are intended to summarize the most general and representative characteristics of the electronic structure of the polyanions by highlighting the major atomic contributions to the molecular orbitals.

The electronic structures of the two isomers are, in qualitative terms, largely similar. Two sets of energy levels, separated by a gap of approximately 10 eV, are observed. The levels in the low-lying set correspond to predominantly nonbonding combinations of s(O) orbitals, whereas the high-lying set contains two (overlapping) bands describing the Mo–O bonding interactions (central band in Figure 2b,c), these being largely d(Mo)–p(O) in character, and also levels that represent nonbonding combinations of p(O) orbitals (upper band in Figure 2b,c).

**Lowest Unoccupied Levels.** A classification scheme for polyoxometalates, based on the number of terminal M–O bonds at the metal centers, has been proposed by Pope<sup>1,2</sup> and has frequently been used for the rationalization of redox behavior. The vast majority of polyoxoanion structures (based on MO<sub>6</sub> units) contain no more than two unshared O atoms in each polyhedral unit and are classified as type-I if there is one terminal M–O bond, or as type-II if two such bonds are present in a cis spatial arrangement. The  $\alpha$  form of  $[\text{Mo}_8\text{O}_{26}]^{4-}$  is an example of a type-II system (the four-coordinate Mo atoms are ignored), but the  $\beta$  isomer formally contains both sorts of octahedra. Therefore, Nomiya and Miwa<sup>3</sup> have described it as a type-III cluster. However, Tytko and co-workers<sup>27</sup> have considered that the  $\beta$ -octamolybdate anion is a type-II species, because the formally two-coordinate O4 atoms behave as pseudoterminal sites.

The redox behavior of type-II systems, unlike that of type-I species, is relatively limited, as electron-transfer processes in these species are normally irreversible and difficult.<sup>2</sup> This

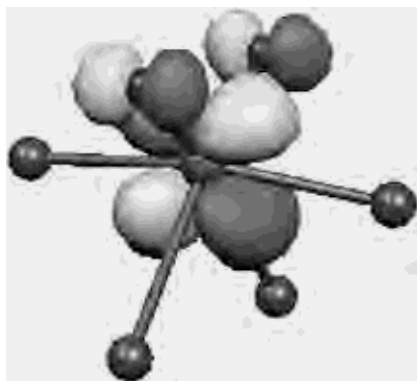


**Figure 3.** Spatial representation of the LUMO ( $7b_1$  orbital) in the *cis*- $[\text{MoO}_2\text{Cl}_4]^{2-}$  complex.

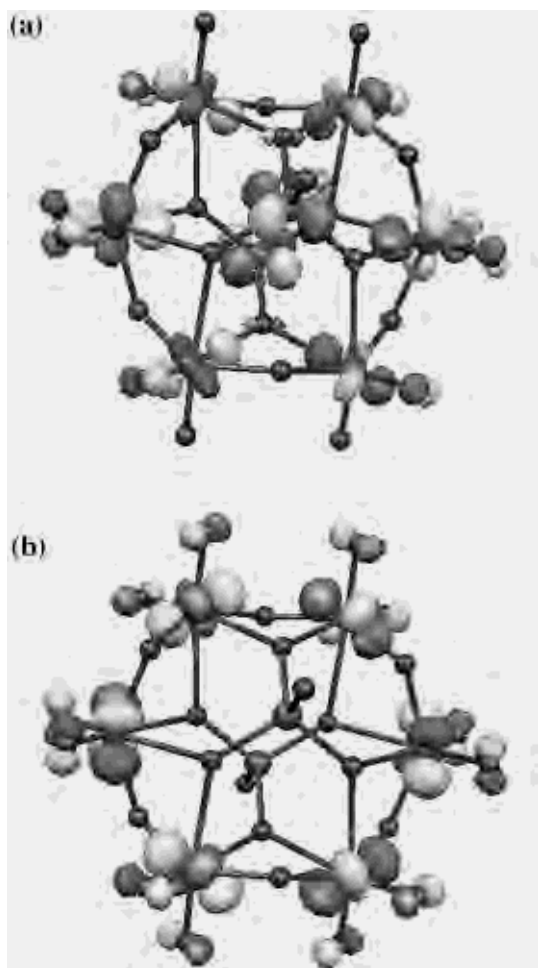


**Figure 4.** Spatial representation of the lowest unoccupied orbitals in the  $\alpha$  isomer: (a)  $23e_u$  and (b)  $9a_{1u}$  orbitals.

has been commonly interpreted using *cis*- $[\text{MO}_2\text{L}_4]$  complexes as models for the individual  $\text{MO}_6$  units in the polyanions.<sup>1,2,8</sup> The M–O antibonding nature of the lowest unoccupied level (LUMO) in the oxidized *cis* di-oxo species has been associated with the observed difficulties in the reduction of type-II polyoxometalates.

Recent calculations<sup>28</sup> have revealed that the LUMO of the *cis*- $[\text{MoO}_2\text{Cl}_4]^{2-}$  complex corresponds to  $\pi$ -like antibonding

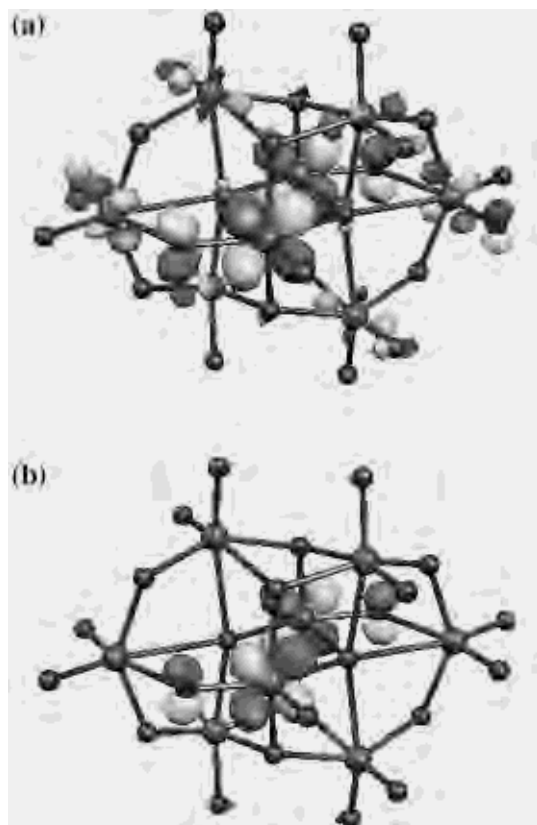


**Figure 5.** Spatial representation of the lowest unoccupied orbitals in the  $\beta$  isomer: (a)  $28b_g$  and (b)  $28a_u$  orbitals.

interactions between  $d_{xz}(\text{Mo})$  and  $p_x(\text{O})$  orbitals (Figure 3). The present results indicate that the LUMOs in the  $[\text{Mo}_8\text{O}_{26}]^{4-}$  anions are the  $23e_u$  and  $28b_g$  levels for the  $\alpha$  and  $\beta$  isomers, respectively (Figure 2). Spatial plots for these orbitals are given in Figures 4 and 5 and show that, as in the model complexes, they can be characterized (predominantly) as an interaction of  $\pi$ -antibonding nature between metal and terminal oxygen atoms.

In the  $\alpha$  form, the LUMO involves both  $\text{Mo}_{6c}$  and  $\text{Mo}_{4c}$  centers, and it is the second lowest unoccupied orbital that corresponds more closely with the LUMO of *cis*- $[\text{MoO}_2\text{Cl}_4]^{2-}$  (Figure 4). In the  $\beta$  form, the first two lowest virtual orbitals are observed to incorporate significant contributions from  $\text{M1}-\text{O}_{\text{pt}}$  interactions (Figure 5), in addition to “normal”  $\text{M}-\text{O}_t$  bonds. This is consistent with the fact that the structural parameters of  $\text{M1}-\text{O}_{\text{pt}}$  bonds are similar to those of terminal bonds (despite the  $\text{O}_{\text{pt}}$  atoms being formally two-coordinate, as noted in the preceding section).

**Closed Loops.** It has been pointed out in the Introduction that Nomiya and Miwa have developed the idea, and quantified it through the index defined by eq 1, of the importance of metal–oxygen interactions along closed loops as a structural stability factor in polyoxometalates. The  $\alpha$  and  $\beta$   $[\text{Mo}_8\text{O}_{26}]^{4-}$  structures have been assigned an equal stability index ( $\eta = 1$ ) from application of eq 1. This result has been obtained by considering one 12-membered  $[\text{Mo}_6\text{O}_6]$  closed loop in the  $\alpha$  isomer and two 8-membered  $[\text{Mo}_4\text{O}_4]$  closed loops in the  $\beta$  isomer.

The bonding mode associated with the  $[\text{Mo}_6\text{O}_6]$  rings in  $\alpha$ - $[\text{Mo}_8\text{O}_{26}]^{4-}$  involves the  $\text{Mo}_{6c}$  and  $\text{O}_{2c}$  atoms and occurs

(28) Bridgeman, A. J.; Cavigliasso, G. *J. Chem. Soc., Dalton Trans.* **2001**, 3556.

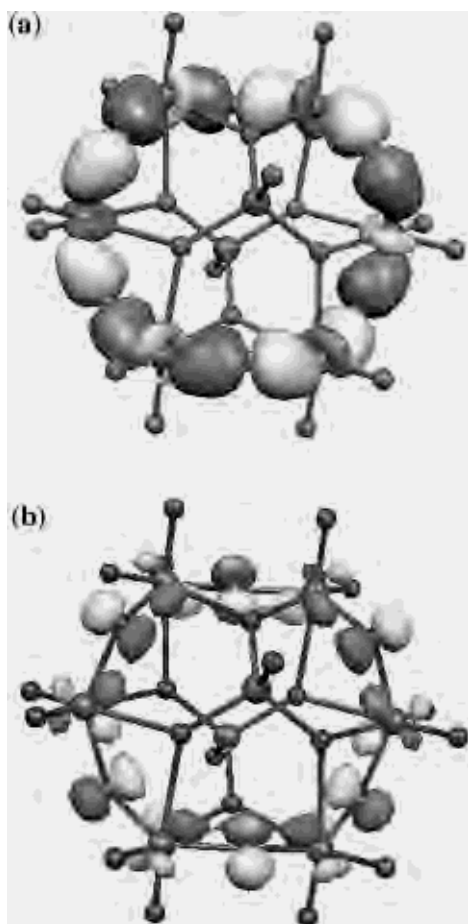


**Figure 6.** Spatial representation of (a)  $\sigma$  ( $4a_{1u}$  orbital) and (b)  $\pi$  ( $10a_{2u}$  orbital)  $[\text{Mo}_6\text{O}_6]$  closed loops in the  $\alpha$  isomer.

in several molecular orbitals, two of which are shown in Figure 6. The  $4a_{1u}$  orbital, part a, is an example of a  $\sigma$ -like interaction, whereas the  $10a_{2u}$  orbital, part b, contains a ring generated via  $\pi$ -like bonds.

The original description<sup>3</sup> of the closed loops in the  $\alpha$  isomer does not include the three-coordinate O atoms (that lie in trans-to-oxo configuration) and the four-coordinate Mo sites (that are treated as “heteroatoms”). However, the spatial plots of the  $11e_g$  and  $12e_u$  orbitals in Figure 7 show that a  $[\text{Mo}_3\text{O}_3]$  ring comprising  $\text{O}_{3c}$ ,  $\text{Mo}_{4c}$ , and  $\text{Mo}_{6c}$  centers can be formulated. The  $\text{Mo}_{6c}\text{--O}_{3c}$  bonds are longer and weaker than analogous (trans-to-oxo) M–O interactions in other isopolyanions (for example, those involving the bridging oxygen atoms in the  $[\text{W}_4\text{O}_{16}]^{8-}$  species<sup>29</sup>), but the symmetry properties of the orbitals presented in Figure 7 suggest that both  $\sigma$  and  $\pi$  bonding modes between  $\text{Mo}_{6c}$  and  $\text{O}_{3c}$  sites are possible.

Nomiya and Miwa have proposed two  $[\text{Mo}_4\text{O}_4]$  rings for the  $\beta$ - $[\text{Mo}_8\text{O}_{26}]^{4-}$  anion but have not provided a description of the structures. Presumably, these rings involve the M1–O6–M3 and M2–O5–M3 bridges and thus satisfy the apparent condition that no M–O bonds in trans configuration with respect to terminal oxygen atoms should be included. Examples of this type of closed loop are given in Figure 8a,b, where the  $20b_u$  ( $\sigma$ -like) and  $14b_g$  ( $\pi$ -like) orbitals are plotted.

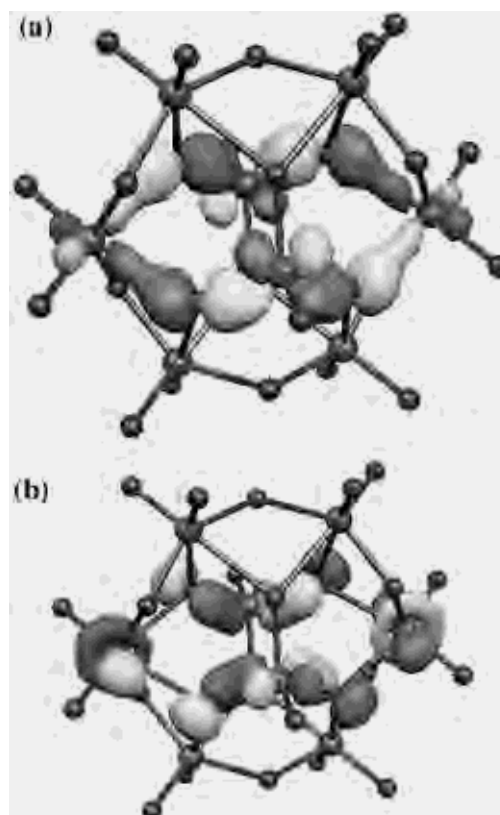


**Figure 7.** Spatial representation of (a)  $\sigma$  ( $11e_g$  orbital) and (b)  $\pi$  ( $12e_u$  orbital)  $[\text{Mo}_3\text{O}_3]$  closed loops in the  $\alpha$  isomer.

As discussed for the  $\alpha$  isomer, the description of closed loops in the  $\beta$  form can also be extended if the possible participation of trans-to-oxo bonds in the construction of rings is not disregarded. For example, Figure 8c,d contains spatial representations of  $\sigma$  and  $\pi$  interactions along an eight-membered  $[\text{Mo}_4\text{O}_4]$  loop with a different connectivity pattern from those involving O5 and O6 sites. This structure consists of M1–O4–M2 and M1–O7–M2 bridges, and the plots correspond to the  $21b_u$  and  $19a_u$  orbitals, respectively.

**Bonding Energetics.** The results of calculations at the BP86 and B3LYP levels of theory favor the  $\alpha$  structure over the  $\beta$  structure by, respectively,  $-101$  kJ/mol (1.05 eV) and  $-149$  kJ/mol (1.54 eV). Further insight can be obtained if the molecular bonding energy ( $E_B$ ) is decomposed as

$$E_B = E_O + E_P + E_E \quad (2)$$

where  $E_O$ ,  $E_P$ , and  $E_E$  are, respectively, orbital mixing, Pauli repulsion, and electrostatic interaction terms. Descriptions of the physical significance of these properties have been given by Landrum, Goldberg, and Hoffmann,<sup>30</sup> and by Baerends and co-workers.<sup>10,31</sup> Both  $E_O$  and  $E_P$  represent orbital interaction effects, but the former is stabilizing whereas the latter is destabilizing. The  $E_E$  contribution is primarily dominated by the nucleus–electron attractions and therefore has a stabilizing influence.

(29) Bridgeman, A. J.; Cavigliasso, G. *Polyhedron* **2001**, *20*, 3101.

(30) Landrum, G. A.; Goldberg, N.; Hoffmann, R. *J. Chem. Soc., Dalton Trans.* **1997**, 3605.

(31) Bickelhaupt, F. M.; Baerends, E. J. *Rev. Comput. Chem.* **2000**, *15*, 1.

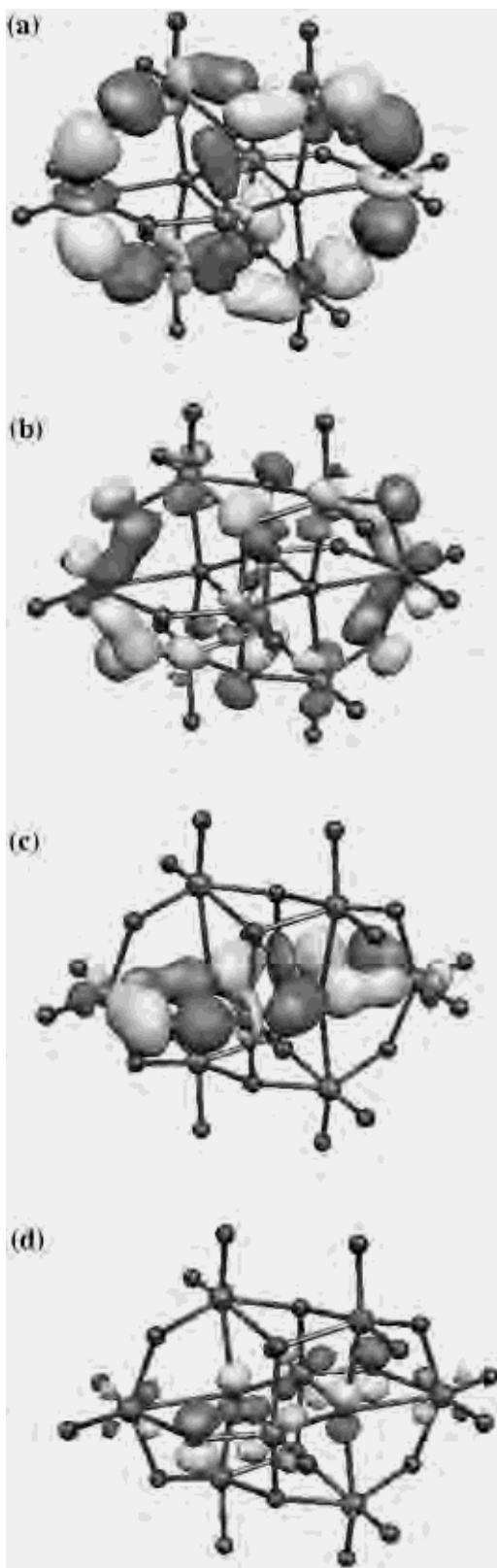


**Figure 8.** Spatial representation of  $[\text{Mo}_4\text{O}_4]$  closed loops in the  $\beta$  isomer: (a)  $20b_u$ , (b)  $14b_g$ , (c)  $21b_u$ , (d)  $19a_u$  orbitals.

Results obtained by applying eq 2 to the  $[\text{Mo}_8\text{O}_{26}]^{4-}$  anions are given in Table 2. The orbital mixing and electrostatic effects are more favorable in the  $\beta$  form. Nevertheless, the Pauli repulsion is of smaller magnitude in the  $\alpha$  form and appears as the dominant stability factor. The Pauli contribu-

**Table 2.** Bonding Energetics (in eV) for the  $\alpha$  and  $\beta$  Isomers of  $[\text{Mo}_8\text{O}_{26}]^{4-}$  <sup>a</sup>

isomer	$E_O$	$E_E$	$E_P$	$E_B$
$\alpha$	-656.72	-215.19	+599.39	-272.52
$\beta$	-662.34	-221.41	+612.28	-271.48

<sup>a</sup> Results correspond to BP86 calculations.

**Table 3.** Mulliken Charges for Mo and O Atoms

isomer	atom	charge
$\alpha$	$\text{Mo}_{4c}$	2.27
	$\text{Mo}_{6c}$	2.10
	$\text{O}_{3c}$	-0.95
	$\text{O}_{2c}$	-0.92
	$\text{O}_t$ (O4)	-0.77
	$\text{O}_t$ (O6)	-0.70
$\beta$	$\text{Mo}_1$	2.24
	$\text{Mo}_2$	2.04
	$\text{Mo}_4$	2.09
	$\text{O}_{5c}$	-1.08
	$\text{O}_{3c}$	-0.99
	$\text{O}_{2c}$ (O5)	-0.90
	$\text{O}_{pt}$ (O4)	-0.81
	$\text{O}_t$	-0.69

tion provides a measure of steric interactions,<sup>31</sup> and the “more open” structure of the  $\alpha$  species seems to be of major importance in this case.

The Mo–O parameters in the  $[\text{Mo}_8\text{O}_{26}]^{4-}$  isomers are rather similar, for all types of Mo–O bonds, but the  $\beta$  structure appears to be somewhat more compact and more sterically crowded than the  $\alpha$  structure, as it contains a greater number of Mo–O bonds. These characteristics should lead to more extensive overlap of the charge distributions and orbitals, which is reflected by the larger calculated values of the bonding energy components.<sup>31</sup>

These results do not support, completely, the original ideas presented by Nomiya and Miwa.<sup>3</sup> The total bonding energy values of the individual isomers are largely similar, the difference being less than one percent, but the orbital mixing effects appear to make a greater contribution to the stability of the  $\beta$  form, which is the structure showing the smaller total bonding energy.

**Population Methods.** The results presented in this section are based on Mulliken and Mayer methodology. These methods are known to exhibit basis set dependence, but (relative) Mulliken charges and Mayer bond indexes can nonetheless provide valuable chemical information for inorganic systems, if uniformity and consistency of the basis sets are maintained.<sup>32</sup> Furthermore, Mulliken analysis has been described as “not an arbitrary choice. . . but consistent with the internal structure of the molecular-orbital formalism”.<sup>22</sup>

**Mulliken Analysis.** Mulliken charges for all atoms and metal basis function populations are given in Tables 3 and 4. The results for the metal atoms correspond to approximately  $d^4$  electronic configurations, in contrast to the formal  $d^0$  assignment, and the charges are considerably smaller than the formal oxidation states. The s and p orbitals are largely unpopulated, in accordance with the molecular

(32) Bridgeman, A. J.; Cavigliasso, G.; Ireland, L. R.; Rothery, J. J. *Chem. Soc., Dalton Trans.* **2001**, 2095.

**Table 4.** Populations of Mo Basis Functions, Given as Percentage Per Individual Orbital

isomer	atom	s	p	d
$\alpha$	Mo <sub>4c</sub>	0.0	1.6	19.0
	Mo <sub>6c</sub>	0.0	1.3	19.2
$\beta$	Mo1	0.0	1.4	19.2
	Mo2	0.0	1.4	19.2
	Mo4	0.0	1.3	19.2

**Table 5.** Mayer Indexes for Mo–O Bonds<sup>a</sup>

isomer	bond	index		
$\alpha$	Mo <sub>4c</sub> –O <sub>t</sub>	1.57	(1.53)	
	Mo <sub>6c</sub> –O <sub>t</sub>	1.65	(1.60)	
	Mo <sub>6c</sub> –O <sub>2c</sub>	0.68	(0.99)	
	Mo <sub>4c</sub> –O <sub>3c</sub>	1.01	(1.32)	
$\beta$	Mo <sub>6c</sub> –O <sub>3c</sub>	0.19	(0.31)	
	Mo–O <sub>t</sub>	1.65	(1.58)	
	Mo–O <sub>pt</sub>	M1–O4	1.25	(1.39)
		M2–O4	0.20	(0.50)
	Mo–O <sub>2c</sub>	M2–O5	0.64	(0.99)
		M3–O5	0.70	(1.01)
	Mo–O <sub>3c</sub>	M1–O6	0.59	(0.90)
		M3–O6	0.53	(0.85)
		M3–O6	0.25	(0.35)
	Mo–O <sub>5c</sub>	M1–O7	0.41	(0.67)
		M1–O7	0.25	(0.33)
		M2–O7	0.17	(0.21)
		M3–O7	0.26	(0.35)

<sup>a</sup> Results from classical bond valence analysis are given in parentheses.

orbital analysis indicating almost exclusive participation of d(Mo) functions in Mo–O bonding.

The negative charge is distributed over all types of oxygen atoms, and the individual values are observed to increase with the coordination number. It is also interesting to note that, although these atoms display the smaller values, the terminal and pseudoterminal sites are significantly charged and collectively bear a comparable proportion of the total negative charge to that accepted by the bridging atoms.

**Mayer Analysis.** Mayer bond order indexes are given in Table 5. Also included are the results obtained with a bond valence model based on the following relationship<sup>27</sup>

$$\log s = \frac{(d_0 - d)}{B} \quad (3)$$

where  $s$  is the bond valence,  $d_0$  is the single-bond length,  $B$  defines the slope of the bond length–bond valence functions, and  $d$  is a calculated bond distance.

For all types of Mo–O interactions, the computational indexes compare well with the bond valence values. The best agreement is found for the shortest and longest bonds, namely, those involving terminal or pseudoterminal O atoms and those characterized by Mo–O distances greater than 230 pm. Deviations for bonds that fall into the intermediate distance range are somewhat larger ( $\sim 0.3$  units) but are typically observed results for metal–oxygen bonds in oxo-anions.<sup>21,33,34</sup> In general, the relative values of the Mayer index for the different bonds follow the trend that would be predicted by a comparison of the corresponding Mo–O distances.

(33) Bridgeman, A. J.; Cavigliasso, G. *Inorg. Chem.* **2002**, *41*, 1761.

(34) Bridgeman, A. J.; Cavigliasso, G. *J. Chem. Soc., Dalton Trans.* **2002**, 2244.

**Table 6.** Covalency and Full Valency Indexes for Oxygen Atoms

isomer	atom	covalency	full valency
$\alpha$	O <sub>3c</sub>	1.80	2.21
	O <sub>2c</sub>	1.82	2.21
	O <sub>t</sub> (O4)	2.01	2.27
	O <sub>t</sub> (O6)	2.07	2.29
$\beta$	O <sub>5c</sub>	1.57	2.13
	O <sub>3c</sub>	1.72	2.17
	O <sub>2c</sub> (O5)	1.85	2.21
	O <sub>pt</sub> (O4)	1.92	2.22
	O <sub>t</sub>	2.09	2.29

The terminal bonds exhibit significant multiple character, but the index is appreciably smaller than the maximum possible covalency as ionic contributions are an important factor in Mo–O<sub>t</sub> interactions. The molecular orbital structure of several bonds involving bridging oxygen sites shows both  $\sigma$  and  $\pi$  character, but the fact that these Mo–O<sub>b</sub> interactions are approximately single or low-order rather than multiple bonds (according to the Mayer analysis) reflects the effects of electron delocalization, which in many cases occurs along the [Mo<sub>n</sub>O<sub>n</sub>] closed loops.

The pseudoterminal atoms in the  $\beta$  isomer have been described as being formally two-coordinate but with properties that are more typical of terminal than bridging bonds (Mo–O<sub>pt</sub> distances in particular). The Mayer index for M1–O4 bonds is approximately twice as large as it is for Mo–O<sub>2c</sub> bonds and indicates some degree of multiple character, but this is smaller than that of actual terminal bonds. These observations suggest that O<sub>pt</sub> atoms are closely related but not equivalent to O<sub>t</sub> atoms. The different behavior can be explained by considering that the contribution from the second Mo–O<sub>pt</sub> (M2–O4) bond, although small, cannot be neglected.

The Mo<sub>4c</sub>–O<sub>3c</sub> index in the  $\alpha$  isomer appears, to some extent, unexpectedly low when compared with results for terminal bonds or from the bond valence model. This is in part related to the longer Mo<sub>4c</sub>–O<sub>3c</sub> than Mo–O<sub>t</sub> distances and to the effect of the additional bonds to the O<sub>3c</sub> atoms, but it also seems to be associated with a relatively stronger ionic contribution, which is reflected by a further reduction in the bond order value.

**Oxygen Valency.** Covalency and full valency indexes for the oxygen atoms are shown in Table 6. The former are calculated as a sum of all Mayer indexes for a particular atom (and therefore include some contributions, for example O–O interactions, that may be small but not necessarily negligible), whereas the latter are a combined measure of covalent (covalency) and ionic (electrovalency) bonding based on Mayer and Mulliken results.

An interesting structural feature of polyoxoanions is the presence of noticeably long M–O bonds in trans configuration with respect to terminal groups. This phenomenon has been normally described as a manifestation of the strong trans influence of the multiply bonded oxo sites,<sup>2</sup> and it is illustrated by the properties of the M6–O3 bonds in the  $\alpha$  isomer, and of the M2–O4, M3–O6, and M–O7 bonds in the  $\beta$  isomer.

Tytko and co-workers<sup>27</sup> have pointed out that, although some or all of their bonds to metal atoms can be rather weak

(individually), the oxygen atoms in trans-to-oxo configurations are not weakly bound sites in polyoxometalates. This is reflected by the results in Table 6. In both the  $\alpha$  and  $\beta$  forms of  $[\text{Mo}_8\text{O}_{26}]^{4-}$ , the differences in the total covalency values are relatively small, and the full valency results suggest that the overall bonding capacities are comparable, despite the variety of bond properties and coordination environments of the oxygen sites.

The oxygen atoms that are affected by trans influence effects can utilize several mechanisms to counterbalance this (in principle) unfavorable situation. In the  $\beta$  isomer, the  $\text{O}_{5c}$  atoms adopt a high-coordination environment, and the  $\text{O}_{pt}$  ( $\text{O}_4$ ) atoms form a strong pseudoterminal ( $\text{M1}-\text{O}_4$ ) bond. In the  $\alpha$  isomer, the  $\text{O}_{3c}$  atoms combine both mechanisms in being relatively high-coordinate and having a rather strong interaction with the  $\text{Mo}_{4c}$  centers.

### Conclusion

The molecular and electronic structures of the  $\alpha$  and  $\beta$  isomers of  $[\text{Mo}_8\text{O}_{26}]^{4-}$  isopolyanions have been calculated using density functional theory. The structural and bonding properties are in reasonably good agreement with experimental data and bond valence descriptions for these species.

The molecular orbital and population analyses have indicated that Mo–O interactions are predominantly  $d(\text{Mo})-p(\text{O})$  in character, and the Mo (Mulliken) electronic configurations and charges have been found to differ significantly from formal values. Closed loops involving metal and bridging oxygen atoms with both  $\sigma$  and  $\pi$  bonding properties

have been observed. However, it has been found that more orbital rings than those originally proposed by Nomiya and Miwa are possible and that the connection between closed loops and stability is not completely supported by the present calculations on the isolated  $\alpha$  and  $\beta$  forms.

The population results suggest that the negative charge is distributed over all types of oxygen sites (Mulliken analysis), that the terminal bonds possess fractional (not maximized) multiple character and the bridging bonds are of approximately single or low-order character (Mayer analysis), and that the overall bonding capacities of the various oxygen atoms are similar (valency analysis). Thus, although the methodology is not directly related, these computational results are comparable, on a qualitative basis, to the observations made by Tytko and co-workers in their bond valence analysis of polyoxometalates.<sup>27,35</sup> These authors have considered that the acceptance of negative charge by  $\text{O}_t$  and  $\text{O}_{pt}$  sites and the nonmaximization of  $\text{M}-\text{O}_t$  covalency should play an important role in polyoxometalate structures, and they have pointed out that oxygen atoms involved in (individually) weak trans-to-oxo bonds can nonetheless be strongly bound overall.

**Acknowledgment.** The authors would like to thank EPSRC, the Cambridge Overseas Trust, Selwyn College (Cambridge), and the University of Hull for financial support, and the Computational Chemistry Working Party for access to computational facilities in the Rutherford Appleton Laboratory.

(35) Tytko, K. H. *Struct. Bonding (Berlin)* **1999**, 93, 67.